THE MAGNET SYSTEM OF THE ELECTRON POSITRON ACCUMULATOR (EPA)

D. Cornuet
PS Division, CERN, 1211 Geneva 23, Switzerland

Abstract

After two years of operation the magnet system of the Electron Positron Accumulator (EPA) proves to be reliable and well adapted within the specified range of energy between 500 MeV and 650 MeV and even beyond. It includes 16 combined-function dipoles, 48 quadrupoles of three different types grouped in five families, and 12 sextupoles distributed in two families.

Particular emphasis is placed on the design of the saturated combined-function bending magnet. The smooth compensations of the saturation effects and of the end field both optimized at 600 MeV allowed operation down to 400 MeV.

Introduction

The Electron Positron Accumulator is an integral part of the LEP injector chain and acts as a buffer between the e± sources and the PS and SPS synchrotron accelerators [1]. When the LEP project was approved in 1982, a condition was the closure of the Intersection Storage Rings (ISR) at the end of 1983. Thus 44 quadrupole magnets of two types have been recuperated for the injection and ejection transfer lines, for the two focusing families of the F_1DDF_2 structure of the four arcs and for the focusing quadrupoles (referenced F_3' in Fig. 1) near the two high beta insertion zones.

But 28 new quadrupoles of a same type were developped for the two families of the three F_3DDF_3 structure of the two straight lines and the family of the trimming quadrupoles (referenced F_4) which is necessary to adjust at various energies the defocusing strength of the combined-function bending magnets which does not vary proportionally to the energy due to the saturation effect. For the purpose of adjustment of the damping partition numbers and of the normalized transition energy, the lattice imposed combined-function bending magnets with the highest possible field to reduce damping time. 16 combined-function bending magnets have been specially designed and optimized for the energy of 600 MeV with an induction of 1.4 T at the center gap of 45 mm and a defocusing gradient of - 1.19 T/m in the pole profile. The integrated end field is 14 % of the total, so careful shimming and measurement of each magnet is needed.

For the purpose of optimal design and exploitation costs, the current density of all the magnets has been chosen lower than 4.6 A/mm^2 for the energy of 650 MeV. For reliable operation a safety margin of 10 % with respect of the nominal current at 650 MeV was chosen for both the magnets and the power supplies. With such concepts operation has proved very reliable since the beginning of operation in May 1986, and even an accumulation efficiency of 60 % was achieved in 1987 (twice the design value) with positrons at 500 MeV, the main optics functions being in very good agreement with the calculated ones [2].

Combined-function bending magnets

Design - The specified gradient of the type I combined bending magnets being low, symmetric "H"-type magnetic circuit is chosen. The magnets are lighter than "C"-type magnets, cheaper and more stable under electromagnetic forces. The magnet assembly is straight with parallel ends. The 1.5 mm thick laminations made of very low carbon steel (< 20 ppm) are welded in a straight compact assembly with parallel end. Although the high bending angle of the beam trajectory (22° 5) and the low radius of curvature (1.43 m when compared to a yoke length of 0.51 m) lead to increase the pole width of 10 % when compared to curved cores, a lower price is obtained because of the simplicity of manufacture of the yoke and the coils. The coil configuration is cheap with two double pancakes per pole. Moreover, the same type of coils is used for the 14 pure bending magnets (called type II) of the EPA transfer lines. The cross-section of the copper conductors, the number of turns, the pole height and the return yoke thickness have been optimized taking into account the following criteria: current between 400 and 600 A (optimal value for medium range power supplies), ampere-turn drop due to magnetization of the magnetic circuit lower than 5 % (distribution by half in the pole and half in the return yoke), prices of the materials for coils and for the yoke approximately equal.

Poletip. For a specified gradient of - 1 T/m the computer program MAGNET [3] led to increase that gradient of 7 % to compensate gradient drop due to saturation effects and 12 % more to compensate the smaller gradient effective length with respect to the bending effective length. The value of the chosen gradient of - 1.19 T/m was small enough to allow to approximate the hyperbola by a straight line according to equation

$$y = 22.5 + 0.0190718\ x \text{ mm}, \quad -69.5 \text{ mm} \leq x \leq 69.5 \text{ mm} \quad (1)$$

Within the accuracy of ± 0.02 mm of the laminations the advantage of that simple profile was to simultaneously create a sextupole component of 2 T/m^2 which was estimated to be necessary to compensate the sextupolar component due to saturation of the iron. Shims are included at the edges of the tapered pole, they reduce the half-gap to 20.75 mm on the narrow side and to 23.6 mm on the wide side in such a way that the good field region be widened at 600 MeV and the induction errors be symmetrical at 500 MeV and 650 MeV (Fig. 4).

Construction. In order to reduce the effect of systematic punching errors, the blue-steamed laminations are assembled in packages of ten, to be stacked recto-verso. Furthermore, each magnetic circuit is assembled from a mixture of five groups of laminations, so that the average permeabilities of all the magnets are equal within 1 %. Notches in the 30 mm thick end plates are machined for ease of location of the end shims, so that the length of the pole tip is 480 ± 0.2 mm before shimming.

Shimming and measurement. Environment and shimming of the dipole with parallel ends are very important because the vertical focusing strength due to the effect of the entry and exit faces angles is nearly equal to that of the core of the magnet [4], the vertical focusing due to the shape of the extension of the fringe field must be added (4.6 %), as well as the edge effect due to the variation of the bending effective length with the horizontal position in a variable gap.

The proximity of the nearby quadrupoles was simulated and produced an increase of the integrated field strength of 3.1x10^{-4} because of the diminution of the negative extension of the fringe field created beyond the coil heads which are only 32 mm apart from the median plane.

Only the first magnet was completely measured [5]. The end shims were adjusted in such a way that the integrated field strength measured with a 2 m long straight coil follow the law

$$\int_{-1m}^{+1m} B_i\,dz = 0.78444-0.54622x \qquad \text{T.m} \qquad (2)$$

with an accuracy of $\pm$ 1×10^{-4}.

Because the quality of the steel was better than the one foreseen in the initial calculations (stacking factor higher than 98 % instead of 95 % and permeability at 2 T 10 % higher) the saturation effects are lower than the one expected [6], the gradient drop in the center is only 1 %, the equivalent sextupolar component of the end field is only - 3 T/m^2, the homogeneity spread of the integrated bending strength at different energies of 500, 600 and 650 MeV is twice lower than the one expected for the induction itself (cf. Figs. 4 and 6). Due to the already high permeability at 500 MeV, the homogeneity curve at 400 MeV is alike. The foreseen errors being smaller than expected, they could be easily compensated by the five small plates (thickness adjusted from 5 to 11 mm) which constitute the shims at each pole end and the initial punching tool has not been modified for the whole series. Additionally, a field map in the median plane of the first magnet was measured with a Hall probe. The equivalent transfer matrices obtained from these measurements [7] may be compared advantageously (Table 1) with the matrices deduced from the field map calculated by longitudinal cuts with an accurate 2D program POISSON [3] preferably to less accurate 3D programs. It has to be noted that it is on the basis of those calculated fields that the law (2) of adjustment of all the dipoles has been defined [8], so that the corresponding transfer matrix perturbs as little as possible the EPA lattice.

Table 1. Equivalent transfer matrix coefficients of EPA dipoles

	From calculated fields [9]	From measurements [7]	% change
H_{11}	1.0828442	1.0791121	- 0.35
H_{12}	0.5944241	0.5922085	- 0.37
H_{21}	0.2902838	0.2777314	- 4.52
H_{13}	0.116207	0.1159137	- 0.25
H_{23}	0.4071855	0.4069476	- 0.06
V_{11}	0.8483477	0.8517644	+ 0.40
V_{12}	0.5724209	0.5693045	- 0.55
V_{21}	- 0.4896854	- 0.4821626	- 1.56

The 16 bending magnets are shimmed identical to the first one without environment thanks to the long straight coil so that their integral field strength does not differ more than $\pm$ 1×10^{-4} [5].

Each magnet is pulsed ten times at 581 A, so that they all are delivered in the same magnetic state.

Quadrupole magnets

The pole design of the new type of quadrupoles (families D, F_3 and F_4 in Fig. 1) was based on experience of the ISR quadrupoles [10], i.e. a circle and a tangent for a bore diameter of 130 mm and a yoke length of 300 mm. This profile calculated with MAGNET program [3] proved to be adequate (Fig. 5) without any previous prototype. Moreover, as for the ISR quadrupole no shimming at all was necessary. To reduce the exploitation cost, these quadrupoles are air-cooled, and a current density of 1 A/mm^2 has been chosen to avoid any thermal distorsion of the yoke. Due to the low induction at the pole center (0.09 T), the remanent integrated gradient could represent an error (4 o/oo) which is twice the mechanical accuracy of the yoke. Because the quadrupoles of a same family are powered in series the specified spread of the integrated gradient for a same family was $\pm$ 1 o/oo. Each family was adequately selected by measuring with a 1 m long gradient coils each magnet along its axis, and by demagnetising the quadrupole if necessary.

Sextupole magnets

The ISR sextupoles were too big to be installed in the short available space in the arcs. Fortunately, sextupoles no longer used in the CERN Proton Synchrotron were available. For the new type of sextupoles (families XH and XV in Fig. 1) the existing yoke was too long (27 cm) and had to be shortened. The 3 free convection coils have been replaced by 3 water-cooled coils to obtain the specified strength of 10 T/m at 650 MeV. The laminations are neither glued nor welded but just pressed between cast iron flanges, making easy the shortening of the yoke. The pole tip is a circle (R=36 mm) truncated at the angle of 27^{0}43'42". Although the length of the yoke (22 cm) is only 1.6 times the bore diameter (13.7 cm), the homogeneity of the integrated sextupole strength is very little affected by the effect of the fringe fields (Fig. 7).

Acknowledgements

The author wishes to thank Y. Baconnier, P. Bossard, J.P. Delahaye, H. Kugler and M. Bell for stimulating discussions during the study of the magnets. A. Dind, P. Bigler and M. Zanolli took active part in the drawing of the magnets. Thanks to the careful magnetic measurements and shimmings of G. Suberlucq we can be confident on the characteristics of the installed magnets.

References

[1] J.P. Delahaye and A. Krusche, "The lattice design of EPA", Proceedings of the Particle Conference (1983), Santa Fe, N.M.

[2] J.H.B. Madsen et al., "First experience with LPI" Proc. of the Part. Conf. (1987), Washington, D.C.

[3] Ch. Iselin, "CERN computer center write-ups: MAGNET T600, POISCR T604".

[4] J.P. Delahaye, "Effect and correction of an integrated focusing error strength in the EPA bending magnets", PS/LPI/Note 83-4.

[5] G. Suberlucq and M. Tardy, "Mesures magnétiques des dipôles EPA type I", PS/PSR/Note 86-6.

[6] D. Cornuet, "Premières comparaisons entre les mesures magnétiques de l'aimant de courbure EPA et les programmes de calcul", PS/PSR/Note 84-20.

[7] M. Bell and H. Kugler, "The EPA bending magnet and its representation", PS/LPI/Note 86-01.

[8] M. Bell and J.P. Delahaye, "Particle tracking in the EPA bending magnet", LEP Note 439.

[9] M. Bell and H. Kugler, "EPA lattice parameters and geometry revised", PS/LPI/Note 84-29.

[10] R. Perin, "End effects compensation in the auxiliary magnets of the CERN intersecting storage rings", CERN ISR-MA/70-16.

Table 2 MAGNET PARAMETERS OF EPA AT 600 MeV

Description	Bending magnet	Quadrupoles						Sextupoles	
Type	Type I	ISR old	ISRnew	Type N		ISR new	Type N	Type XN	
Family	B	F_1	F_2	D	F_3	F'_3	F_4	X_H	X_V
Quantity	16	8	8	12	8	4	8	8	4
Strength ($T, T/m, T/m^2$)	1.40 T -1.187 T/m	2.204	2.779	1.135	1.127	1.066	0.418	18.75	18.75
Integrated strength ($T.m, T, T/m$)	0.78444 T.m 0.54622 T	0.8376	1.056	0.407	0.404	0.404	0.15	5	5
Gap height, Bore diam (mm)	45	184	200	130	130	200	130	137	137
good field region (mm)	110	100	100	100	100	160	100	85	85
Current (A)	528	61.3	89.8	40.3	40.0	34.4	14.8	41	41
Power (W)	7600	865	3000	130	128	440	18	168	168

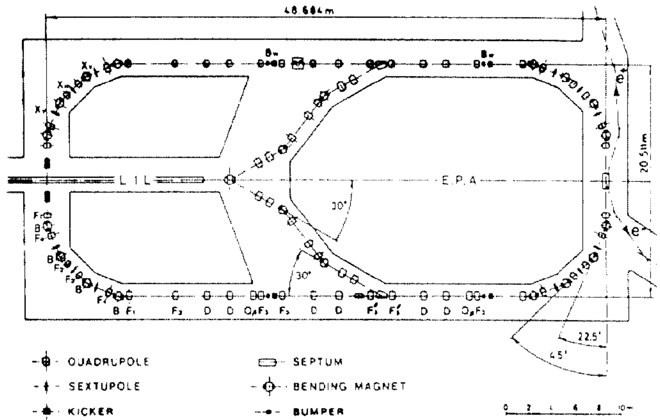

Fig. 1 General EPA layout

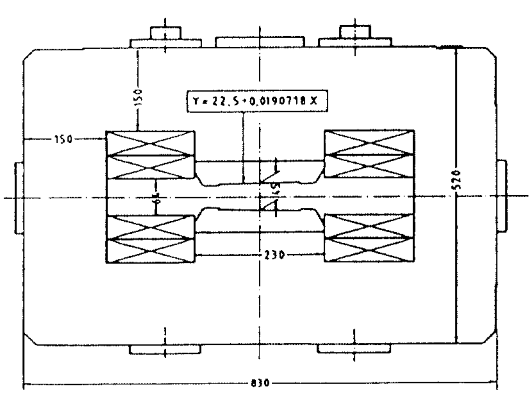

Fig. 2 Cross-section of type I dipole

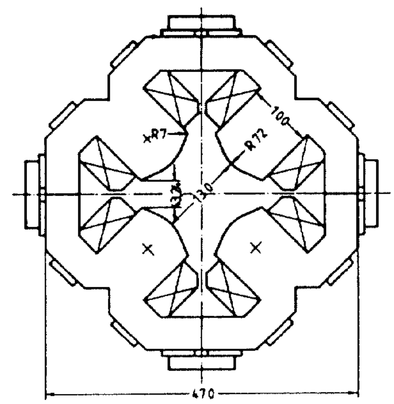

Fig. 3 Cross-section of type N quadrupole

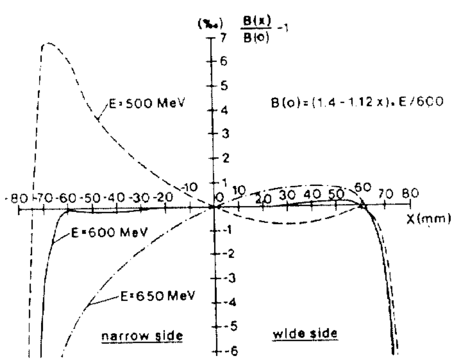

Fig. 4 Type I - Calculated homogeneity curves

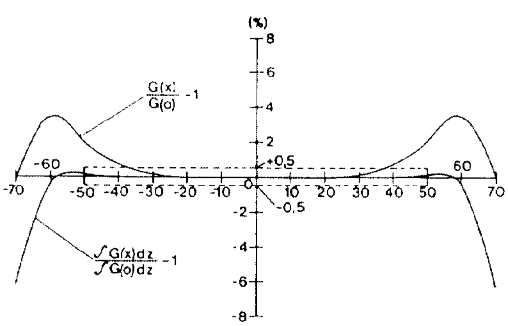

Fig. 5 Type N - Homogeneity curves

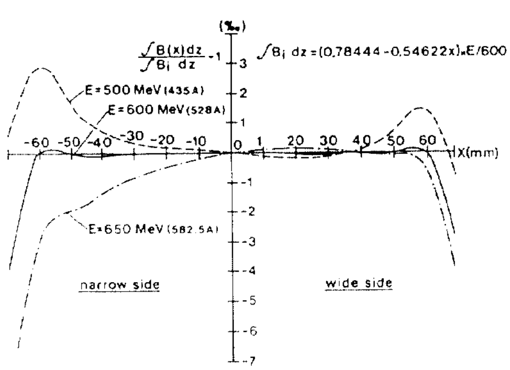

Fig. 6 Type I - Measured homogeneity curves

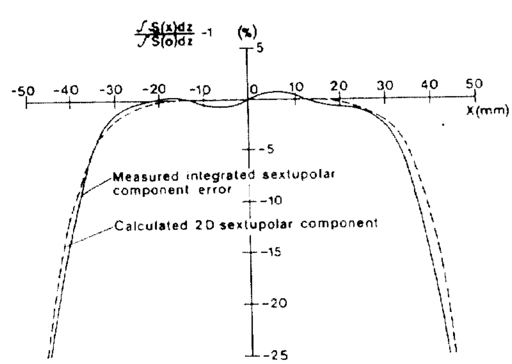

Fig. 7 Type XN - Calculated and measured homogeneity curves